Applied Catalysis A: General 486 (2014) 42–48

Contents lists available at ScienceDirect

Applied Catalysis A: General

journal homepage: www.elsevier.com/locate/apcata

Titanium hydrogenphosphate: An efficient dual acidic catalyst for 5-hydroxymethylfurfural (HMF) production

Md. Imteyaz Alam[a], Sudipta De[a], Bhagat Singh[a], Basudeb Saha[a,b,*], Mahdi M. Abu-Omar[b,**]

[a] Laboratory of Catalysis, Department of Chemistry, University of Delhi, North Campus, Delhi 110007, India
[b] Department of Chemistry and the Center for Direct Catalytic Conversion of Biomass to Biofuels (C3Bio), Purdue University, IN 47907, USA

ARTICLE INFO

Article history:
Received 12 June 2014
Received in revised form 12 August 2014
Accepted 18 August 2014
Available online 23 August 2014

Keywords:
Titanium hydrogenphosphate
Dual acidity
Carbohydrates
5-Hydroxymethyl furfural
Biphasic solvent

ABSTRACT

Dual Brønsted and Lewis acidity of solid acid catalysts enhances selective production of 5-hydroxymethylfurfural (HMF). This report describes a simple template-free synthetic approach for the preparation of titanium hydrogenphosphate (TiHP) material containing Lewis and Brønsted acid sites. As-synthesized material has been thoroughly analyzed by several analytical methods for elucidating its structural properties, including determination of the presence of Brønsted acidic phosphate group and measurement of total acid density. NH_3-TPD data reveals high surface acidity (1.43 mmol g^{-1}) of the TiHP, which is indeed reflects to its catalytic effectiveness for the conversion of fructose, giving 55% HMF in biphasic solvent. Glucose conversion gives better yield (35%) when the reaction was carried out in a larger reactor (2 L Parr reactor), which might be due to better mechanical stirring and hence higher mixing efficiency of the reactants. Brønsted acid sites in the catalyst facilitated the formation of furan ring opening product, levulinic acid, at higher temperatures. The catalyst shows excellent recyclability and the recovered catalyst after the 3rd cycles retained XRD and TGA characteristics.

1. Introduction

Design and synthesis of non-corrosive, environmentally benign and low cost recyclable acidic catalyst is critical to the development of sustainable dehydration process for producing furan-based chemicals from biomass [1–3]. 5-Hydroxymethylfurfural (HMF), a versatile platform chemical, is expected to play a key role as a petroleum replacement precursor for renewable chemicals and biofuels [4,5]. Thus, development of cost effective technologies for HMF production is of great interest. Several process parameters including biomass resources [6–8], reaction media [9–12] and catalysts have been explored to achieve this goal. High boiling point organic solvents and ionic liquids, and homogeneous catalysts have offered some advantages to achieve high HMF yields, but energy intensive separation of solvents and catalysts of these processes poses disadvantages to their commercialization efforts. In this context, the use of heterogeneous catalysts and biphasic solvents are certainly advantageous [13]. Examples of solid acid catalysts used for dehydration reactions includes metal oxides [9,14], magnetically separable materials [15], heteropolyacids [16], zeolites [17], and ion-exchange resins [18]. Metal phosphates are considered as most emerging group of materials of this type because of their highly diverse composition and structures enabling high acidity and surface area [19].

Recently phosphates of Nb [20], Ta [21], Ti [22] and Zr [23] have been synthesized and used as acid catalysts for dehydration of biomass and biomass derived carbohydrates into HMF. Among these phosphates, titanium phosphate (TiP) has received greater attention because of its unique catalytic properties, such as Lewis acidity with tunable acid density, and high life span due to thermal and chemical stability. Applications of layered [24–26], open-framework [27,28] and mesoporous TiP [19,22] as acid catalysts are already known. Yin et al. reported a method for microemulsion-based synthesis for TiP nanotubes *via* amine extraction system in Teflon lined autoclave at 180–200 °C [29]. However, $Ti(HPO_4)_2{\cdot}½H_2O$ material prepared in this method limits its application because of incorporation of intact trioctylamine ($(C_8H_{17})_3N$) into the nanostructure of the phosphate. Synthesis of mesoporous TiP having 124 m^2 g^{-1} surface area and 42 Å pores size has been reported from titanium isopropoxide precursor and

* Corresponding author at: Department of Chemistry and the Center for Direct Catalytic Conversion of Biomass to Biofuels (C3Bio), Purdue University, IN 47907, USA. Tel.: +1 7652377649.
** Corresponding author.
E-mail addresses: sahab@purdue.edu (B. Saha), mabuomar@purdue.edu (M.M. Abu-Omar).

http://dx.doi.org/10.1016/j.apcata.2014.08.019
0926-860X/

polymeric Pluronic P123 surfactant [30]. Significantly higher surface area (740 $m^2 g^{-1}$) was realized when the same material (mesoporous TiP) was prepared from a reaction between phosphoric acid solution and titanium propoxide or titanium chloride in the presence of cationic surfactant [19]. Apart from cationic surfactant, high surface area mesoporous titanium phosphate has also been synthesized using anionic surfactant [31]. Most recently, Dutta et al. [22] developed hierarchical macro/meso-porous titanium phosphate through a slow evaporation method by using titanium isopropoxide and orthophosphoric acid as inorganic sources and Pluronic P123 as a structure directing agent. However, the use of expensive precursors and template molecules, difficulties in removal of template/surfactant, low yield and long reaction time are some drawbacks of these methods. Therefore, a simple method for the synthesis of TiP materials is more desirable.

This paper describes a simple approach for the synthesis of acidic titanium hydrogenphosphate (TiHP), and its catalytic effectiveness for the dehydration of carbohydrate substrate in bi-phasic medium. The said TiHP material is prepared by refluxing commercial TiO_2 and H_3PO_4 at 160 °C without any template molecule, and characterized by FTIR, XRD, HRTEM, CHNS elemental analyzer, TGA and NH_3-TPD methods. As-synthesized TiHP exhibits good catalytic activity for HMF preparation in water/THF biphasic solvent under conventional heating. A comparison of small scale reactions carried out in a 50 mL pressure reactor and a larger scale reaction in 2 L Parr reactor under mechanical stirring reveals that the later reaction gives higher yields because of efficient stirring. Because of high stability and water-tolerant nature of the TiHP, recovered catalyst retained activity upon recycling. Material characterization data of the recovered catalyst compared well with that of as-synthesized material.

2. Experimental

2.1. Materials and instrumentation

TiO_2, D-glucose, D-fructose and galactose were purchased from Thomas Baker (India). H_3PO_4 and tetrahydrofuran were supplied by Fischer Scientific and S D Fine Chemical (India), respectively. Cellobiose and maltose were purchased from Sigma Aldrich. Unless otherwise stated, distilled water was used as an aqueous phase. Fourier transform infrared (FTIR) spectra of TiHP were recorded on a Perkin-Elmer spectrometer (model 1752X FTIR) by using KBr pellet. Powder X-ray diffraction of the TiHP was carried out using a Brucker Advance D-8 machine. Thermo gravimetric analyses (TGA) were performed on a Shimadzu (model DTG-60) thermal analyzer under air at a heating rate of 10 °C min^{-1}. HR-TEM (transmission electron microscopy) images were recorded on a JEOL DATUM Model No. JEM1011. SEM image was analyzed on Hitachi, S-4100 at an accelerating voltage of 20 kV. N_2 adsorption–desorption isotherms were obtained by using a Beckman Coulter SA 3100 Surface Area Analyzer at 77 K. Elementar Analysensysteme GmbH VarioEL V3 elemental analyzer was used for measuring hydrogen content of the TiHP. Temperature programmed desorption (TPD) of ammonia was performed on ALTAMIRA Q-800 instrument equipped with an analyzer and a thermal conductivity detector. In this method, the sample was activated at 450 °C for 2 h in a U-tube glass cell under He flow and cooled to 150 °C. The sample was then saturated with ammonia for 30 min at a rate of 20 mL min^{-1}. After exposure to ammonia, the material was subsequently purged with He to measure desorption of ammonia in the range of 100–900 °C at a heating rate of 10 °C min^{-1}. The catalytic conversions of carbohydrate substrates into HMF were performed in stainless steel Parr reactors. ^{1}H NMR spectral analysis was performed on a JEOL JNM ECX-400 P 400 MHz instrument and data were processed using a JEOL DELTA program version 4.3.6. The yield of HMF was determined from ^{1}H NMR signals with reference to known amount of internal standard. Conversions were calculated by measuring unconverted reduced sugars by phenol sulfuric acid analysis method [32].

2.2. Preparation of TiHP

TiO_2 (1.60 g) and H_3PO_4 (2.45 g) were mixed with distilled water (5 mL) in a round bottom flask. The reaction mixture was heated to reflux with continuous stirring at 160 °C for 8 h using chilled water fitted with a condenser. The mixture was then cooled to room temperature, filtered and washed with hot water until pH of filtrate is neutral. The resultant white solid was oven dried at 65 °C for 12 h. A schematic representation for catalyst preparation is shown in supporting information (Fig. S1).

2.3. General reaction procedure

Small scale experiments were performed in a 50 mL stainless steel reactor equipped with temperature controller, pressure gauge, stirrer and rupture disk. The larger scale reactions (10–30 g substrate) were carried out in a 2 L Parr reactor equipped with mechanical stirrer, pressure and temperature controller, a chillier and rupture disk. In typical small scale experiments, the reactor was charged with NaCl saturated water as a reactive phase, THF as an extracting phase, substrate and catalyst. The reactor head was sealed tightly before heating the reaction mass at the desired temperature for a set time. After completion of reaction, the mixture was allowed to cool down to room temperature. The organic phase was separated in a round bottom flask. The remaining HMF in the aqueous phase was further extracted by ethyl acetate and collected in the round bottom flask. After removing solvent by rotary evaporator under vacuum, crude HMF was analyzed by ^{1}H NMR. The aqueous layer was also analyzed by UV–vis spectrophotometric method for measuring any remaining HMF in the aqueous phase.

2.4. Determination of HMF yield

The yields of HMF in the organic and aqueous phases were measured separately by ^{1}H NMR and UV–Vis spectrophotometric techniques, respectively. Since NaCl saturated aqueous solution was used to increase partition coefficient of the organic products and the reactive phase was washed four times with ethyl acetate, the amount of HMF remaining in the aqueous phase was negligible as compared to the organic phase. Crude HMF, obtained after removal of extracting phase, was analyzed by ^{1}H NMR by using a known amount of mesitylene as internal standard. The yield of HMF was calculated from integrated values of the —CHO proton (δ = 9.58 ppm) of HMF and the three aromatic ring protons of mesitylene (δ = 6.78 ppm) (Fig. S2). The aqueous phase was analyzed directly by UV-Vis spectroscopic technique as HMF has a distinct peak at 284 nm with the corresponding molar extinction coefficient (ε) of 1.66×10^4 M^{-1} cm^{-1}. Unless otherwise mentioned, the reported HMF yields (mol%) are the sum of HMF obtained from both organic and aqueous phases.

3. Results and discussion

3.1. Catalyst characterization

The FTIR spectrum of as-synthesized TiHP material (Fig. 1(a)) shows characteristic band of phosphate group at about 1000 cm^{-1} and a band at 1260 cm^{-1} for P—O—H deformation mode, which are absent in the precursor TiO_2. This comparison suggests that acidic hydrogen phosphate group is successfully incorporated on

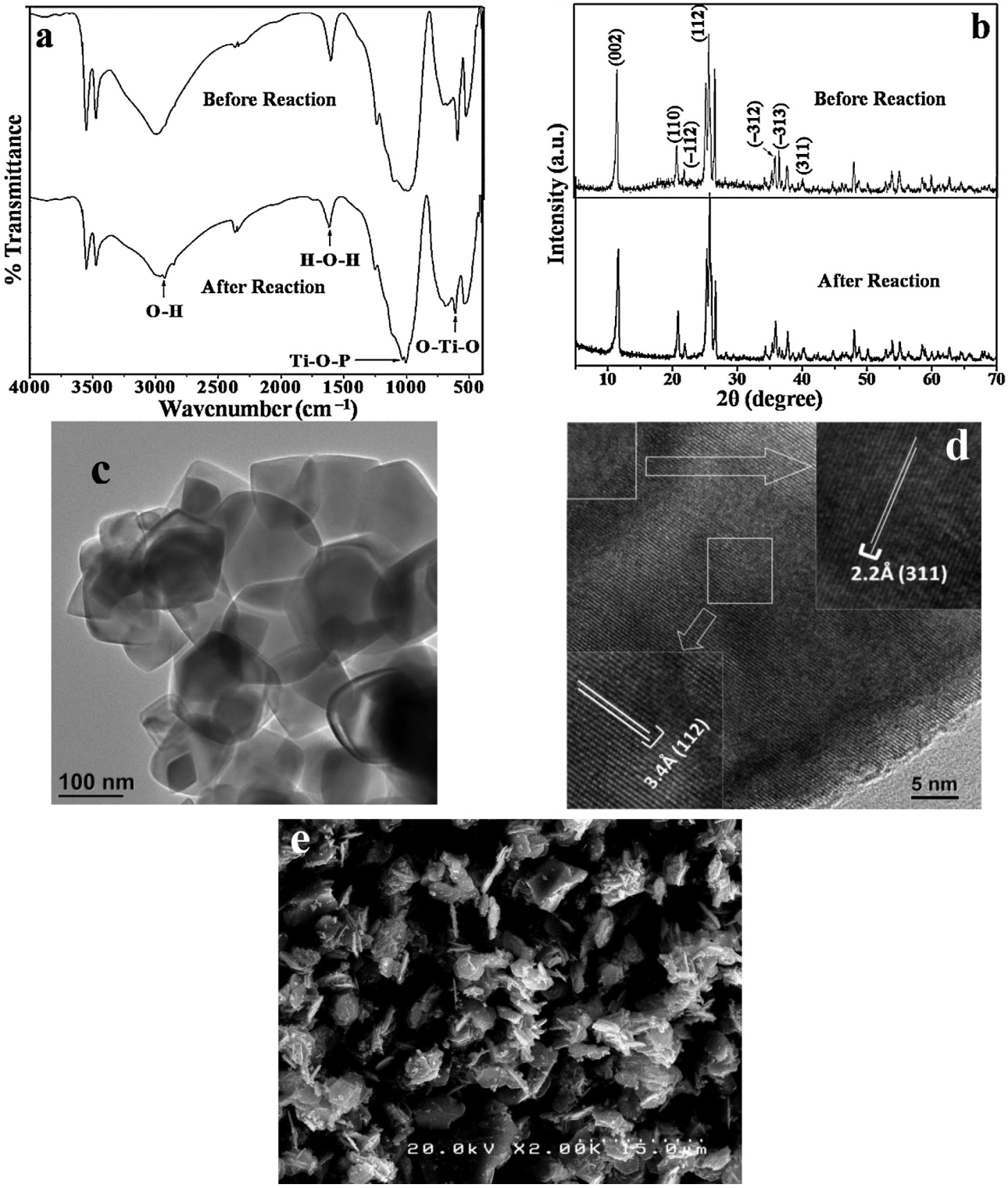

Fig. 1. FTIR spectra (a), powder XRD pattern (b) of as-synthesized and reused TiHP, HRTEM (c), lattice fringes (d) and FESEM image of as-synthesized TiHP.

TiO_2 upon refluxing with phosphoric acid. Similar observation has also been reported in a previous report [33]. The bands at 3554 and 3474 cm^{-1} possibly corresponds to the stretching vibration of —OH group of water presents in the TiHP crystal. The higher vibration frequencies of the doublets could be due to weak hydrogen bonding interaction of water in TiHP structure. The low intense peak near 1620 cm^{-1} can be assigned to the deformation vibration for H—O—H bonds of absorbed moisture [34]. A broad band at 3000 cm^{-1} represents the O—H stretching vibration of the —PO_3—OH groups.

Powder X-ray diffraction (PXRD) was recorded at room temperature with CuKα (λ = 1.54 Å radiation) on a Brucker Advance D-8 diffractometer. Diffraction intensity was measured at a scan rate of 2° min^{-1}. The XRD pattern was analyzed by XPowder12 (ver.01.04) software in order to elucidate the crystalline characteristic of the TiHP. The characteristic peaks at 11.6°, 20.8°, 21.9°, 25.7°, 35.9°, 36.5° and 40.1° with their respective *d*-values of 7.59, 4.26, 4.05, 3.46, 3.46, 2.46 and 2.24 can be indexed to (0 0 2), (1 1 0), (−1 1 2), (1 1 2), (−3 1 2), (−3 1 3) and (3 1 1) reflections (Fig. 1(b)). These 2θ

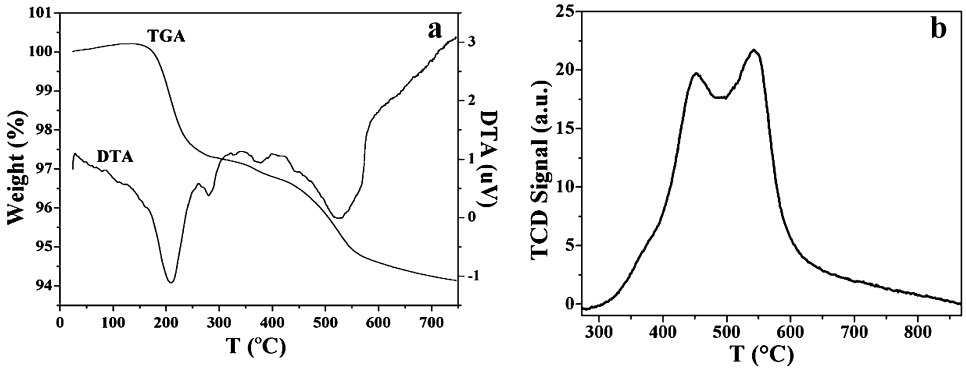

Fig. 2. TGA–DTA profile (a) and NH_3-TPD desorption pattern of the TiHP.

values agrees well with the characteristic peaks of $Ti(HPO_4)_2{\cdot}H_2O$ (JCPDS card No. 033-1379) and a previous literature data [35]. The peak at 25.3° corresponds to unconverted TiO_2. Theoretically, pure $Ti(HPO_4)_2{\cdot}H_2O$ should contain 1.55 and 24 wt% of H and P, respectively. The lower value of actual H (1.03 wt%) and P (11.5 wt%) possibly suggests that the synthesized material is a mixture of $Ti(HPO_4)_2{\cdot}H_2O$ and $Ti(HPO_4)_2{\cdot}½H_2O$ and some unconverted TiO_2 (Fig. S4).

The representative TEM, HRTEM and FESEM images of TiHP are shown in Fig. 1(c)–(e). These TEM images show that most of the particles are of rectangular shape with some of hexagonal and that the particle size varies in the range of 80–120 nm. HRTEM image suggests the material contains characteristic (1 1 2) and (3 1 1) planes as those observed from XRD pattern. FESEM image also shows that this material has hexagonal shaped plate like structure. The BET surface area of the TiHP material, measured by a N_2 adsorption–desorption study at 77 K, shows low surface area ($4.4\ m^2\ g^{-1}$) which could be due to aggregation of the particles. TGA and differential thermal analysis (DTA) data are shown in Fig. 2(a). The data show two distinct mass loss steps corresponding to total loss of about 6%. The first step in the range of 150–260 °C could be due to the loss of water of crystallization. The second weight loss is probably attributed to the condensation of structural hydroxyl (PO_3–OH) groups due to the interaction of hydrogen phosphate groups to produce pyrophosphate (Fig. S3). The observed mass loss steps were further confirmed by DTA curve. Acid density of the TiHP material was quantified by NH_3-TPD measurement. As shown in Fig. 2b, the desorption profile reveals two desorption peak maxima at high temperatures of 455 and 550 °C and the corresponding total acid density is $1.43\ mmol\ g^{-1}$. The high temperature desorption indicates the presence of strong acid sites in the material. The investigated catalyst is believed to contain Brønsted and Lewis acid sites. The Lewis acidic centers are generated from tetravalent Ti^{+4} while the surface P–OH groups represent Brønsted acidity. The Brønsted acidity is also dependant on the bonding nature of P with other atoms in the material and thus the availability of protons. Comparable peak intensity of the two peaks in the desorption profile perhaps suggest that the concentrations of Brønsted and Lewis acid sites are very similar. The total acid density ($1.43\ mmol\ g^{-1}$) is higher than the reported value ($0.711\ mmol\ g^{-1}$) by Jones et al. [19] in which TiP was prepared from a reaction between phosphoric acid solution and titanium propoxide or titanium chloride in the presence of cationic surfactant.

3.2. Catalysis

Acid density is an important parameter of a catalyst for determining overall catalytic effectiveness for dehydration reaction. As total acid density of the TiHP is remarkably high, it is worth to examine its catalytic effectiveness for the conversions of fructose and naturally abundant glucose. A preliminary reaction between 500 mg fructose and 250 mg TiHP at 140 °C for 3 h yielded 55% HMF and converted 80% fructose in water (2 mL)/THF (10 mL) biphasic solvent. The aqueous phase was saturated with 0.6 g NaCl (30 wt%) to ensure distinct phase separation of the two solvents and to improve partitioning of HMF into the organic phase. In the absence of salting-out effect, a reaction without NaCl produced only 38% HMF (Fig. S5). Similar observation of higher partition coefficient of HMF in the presence of NaCl in the aqueous phase is also precedent in the literature [12,36,37]. Under comparable reaction conditions, TiO_2 (precursor for TiHP) catalyzed reaction gave only 5.1% HMF. When a mixture of H_3PO_4 (1 mL of 1 M solution) and 250 mg TiO_2 was used as catalyst, the reaction produced 33% HMF with 96% fructose conversion. This comparison suggests that as-synthesized TiHP catalyst containing both Lewis and Brønsted acid sites is more effective for HMF production than its Lewis acidic component (TiO_2) or a mixture of two acid precursors, which is perhaps due to the occurrence of fructose dehydration inside the catalyst pores [12]. The novelty of the present TiHP catalyst was further realized when its catalytic effectiveness was compared with the activity of the reported metal phosphate catalysts [20,22,37–39]. As shown in Table 1, other metal phosphates catalyzed dehydration of fructose yielded 35–77% HMF. Among the reported metal phosphates, large mesopore Sn-phosphate (LPSnP-1) containing higher acid density ($2.2\ mmol\ g^{-1}$) gave maximum yield (77%) (Table 1, entry 5). Another reason for higher yield of the LPSnP-1 catalyzed reaction is that this reaction was carried out under microwave (MW) heating in contrary to conventional heating in the present reaction. It is known from previous reports that fructose dehydration under MW irradiation yielded significantly higher HMF (30–40%) than the conventional heating [6]. Another reaction using ZrP catalyst (Table 1, entry 2) gave comparable yield to that of the TiHP catalysis, but the former reaction required higher temperature (240 °C) to achieve sub-critical condition. As MW irradiation or sub-critical conditions are not practical approaches for HMF production in scalable quantity, the present catalyst giving maximum 55% HMF under conventional heating condition represents a sustainable approach.

More experiments were designed for optimizing the laboratory scale process conditions by varying the reaction temperature, catalyst dosages and reaction time. The first set of experiments at varying reaction time from 1 to 3 h showed about 2.4 folds increased in HMF yields (23% in 1 h to 55% in 3 h) (Fig. 3). A further increase in reaction time from 3 h to 4 h showed detrimental effect on yields, giving only 41% HMF, whereas the concentration of levulinic acid (LA), a rehydration product of HMF with water [41], increased from 1% to 9%. The temperature variation experiments showed an upward trend of fructose conversions with temperatures, but HMF yields did not follow the same trend (Fig. 4). The yield increased from 17% at 120 °C to 55% at 140 °C, followed by a decreasing trend in yields at higher temperatures. At the same

Table 1
A comparison of catalytic activity of the TiHP with those of reported phosphate materials.

Entry	Catalysts	Acid density (mmol g^{-1})	Solvent	T (°C)	t (min)	HMF yield (%)	Reference
1[a]	NbPO-pH2	0.221	H_2O	130	30	45	[21]
2[b]	ZrP	–	sc-H_2O	240	3	53.5	[38]
3[c]	α-$Cu_2P_2O_7$-900	–	H_2O	200	5	35.8	[39]
4[d]	MTiP-1	–	H_2O-MIBK	140	5^{MW}	35	[23]
5[e]	LPSnP-1	2.2	H_2O-MIBK	150	2^{MW}	77	[37]
6[f]	TiHP	1.4	H_2O-THF	140	180	55	This work

sc: sub-critical; MW: microwave.
[a] Fructose/catalyst = 1:1, P = 0.8 MPa (N_2 gas).
[b] Fructose/catalyst = 1:1, P = 3.35 MPa.
[c] Fructose/catalyst = 10:1, P = 25 bar (N_2 gas).
[d] Fructose/catalyst = 5:1.
[e] Fructose/catalyst = 4.5:1.
[f] Fructose/catalyst = 2:1.

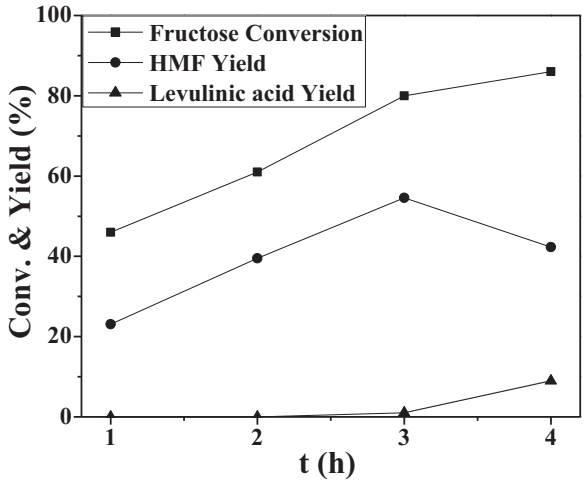

Fig. 3. Reaction profile as a function of reaction time for fructose (500 mg) dehydration with the TiHP (250 mg) catalyst in water/THF (2:10 (v/v)) at 140 °C. The aqueous phase contained 0.6 g NaCl.

time, the concentration of LA increased from 4% at 160 °C to 16% at 170 °C. Previous reports also evidenced of higher LA yields at higher temperatures [41]. It is important to note that total yields of HMF and LA did not change significantly in the temperature range of 140–170 °C, although fructose conversions increased to almost 100%. Therefore, it can be inferred that oligomerization between HMF and fructose that results in the formation of soluble and insoluble humin by-products could account for the observed carbon mass loss [6]. This interpretation was further supported by the fact that the product solution turned dark brown at higher temperatures although these products were not quantified due to analytical issues. At higher temperatures, HMF hydrated to levulinic acid due to the presence of Brønsted acidity in the catalyst.

The effect of catalyst loading on the yield of HMF was also studied by varying catalyst loadings from 100 mg to 400 mg for dehydration of 500 mg fructose at 140 °C for 3 h in water-NaCl/THF solvent (2:10 (v/v)). The yield of HMF increased from 32 to 55% upon increasing the catalyst loading from 100 mg to 250 mg. A further increase in catalyst loading to 400 mg showed no improvement in yields (Fig. S6). The observed non-linearity of HMF yield as a function of catalyst loading could be due to mass-transport limitation involving heterogeneous catalyst. It is also possible that dissolution of fructose in the reactive phase decreased due to the formation of slurry at higher catalyst loading.

The effectiveness of the TiHP catalyst was further tested for difficult monosaccharides, such as glucose, galactose and disaccharides such as cellobiose and maltose. The conversions of these substrates were carried out under comparable reaction conditions of 500 mg substrate, 250 mg catalyst, water-NaCl/THF (1:5 v/v) biphasic solvent and at 140 °C for 3 h. As shown in Fig. 5, HMF yield from glucose (17%) as well as glucose conversion (29%) was significantly lower when compared with fructose dehydration results. Although glucose conversion process involved an additional isomerization step in the reaction progression, a large difference in HMF yields (37%) and substrate conversions (68%) between fructose and

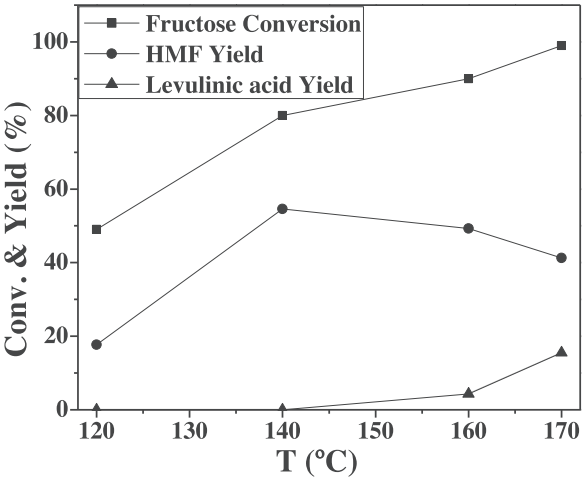

Fig. 4. Reaction profile as a function of temperatures for fructose (500 mg) dehydration with the TiHP catalyst (250 mg) in water/THF (2:10 (v/v)) biphasic solvent for 3 h. The aqueous phase contained 0.6 g NaCl.

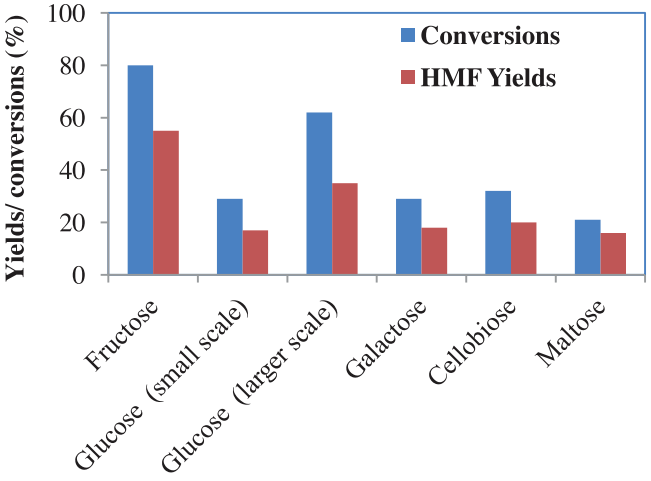

Fig. 5. A comparative analysis for substrate conversions and HMF yields.

glucose must be related to the nature of the catalyst or the process conditions. It is known that Lewis acid facilitates isomerization of glucose to fructose and the Brønsted acid assists dehydration of fructose. This conclusion is based on observation of a previous report in which Sn-beta/HCl catalyzed dehydration of glucose achieved 4-folds HMF yield than the Sn-beta catalyzed reaction [42]. Similar observation has also been reported by Zhao et al. [43] in which the authors used heterogeneous catalysts of varying total acid density containing only Brønsted acidity as well as combined Brønsted and Lewis acid sites. The results showed that the Amberlyst-15 catalyst containing highest acid density, but only Brønsted acid sites, exhibited the lowest HMF yield from fructose as compared with heteropolyacid, $Cs_{2.5}H_{0.5}PW_{12}O_{40}$, catalyst having significantly lower acid density. The later catalyst containing both Brønsted and Lewis acid sites is believed to be responsible for better catalytic activity due to minimization of secondary side reactions involving HMF degradation. However, relative activity of such Lewis–Brønsted catalyst depends on the ratio of Lewis to Brønsted acid sites. In case of TiHP catalyst the ratio of the two acid densities seems equal from the NH_3-TPD desorption pattern; thus, the lower activity for glucose conversion might be limited by the mass-transport of the heterogeneous catalyst in the small reactor. To test this hypothesis, glucose dehydration reaction was carried out in a 2 L Parr reactor. This larger scale reaction between 10 g glucose and 5 g catalyst in water (25 mL)/THF (125 mL) in the presence of 30 wt% NaCl in the aqueous phase produced 27% HMF for 3 h with 59% glucose conversion. Another reaction using 30 g of glucose and 15 g of catalyst in water (75 mL)/THF (375 mL) achieved slightly higher HMF yield (35%) and glucose conversion (62%). The superior results in the later reactions may be due to better mixing of the reactants in the larger reactor with stronger mechanical stirring capability.

Similar to glucose, galactose, a C-2 epimer of glucose, also yielded low HMF (18%). Among the two disaccharides (cellobiose, maltose), cellobiose, the smallest possible repeat unit of cellulose, produced 20% HMF. The conversion of cellobiose, which progresses through hydrolysis of cellobiose to glucose, isomerization of glucose to fructose and finally dehydration of fructose, involved an additional hydrolysis step in the reaction sequence than that of glucose. While cellobiose being a dimer of two glucose units theoretically contains double the amount of glucose, a slightly higher HMF yield from cellobiose than from glucose (based on results suggests that overall HMF yield from cellobiose is perhaps limited by its hydrolysis step. On the other hand, maltose which is also a dimer of two glucose units achieved a slightly lower yield (16%). This slight difference may be due to difference in their hydrolysis rates as two glucose units in cellobiose are bonded through (β(1→4) linkage whereas those in maltose are linked through α(1→4) glycosidic bond. Similar trend of higher HMF product from cellobiose than that from maltose was also observed for $GeCl_4$ catalyzed reaction in ionic liquid at 120 °C [40].

3.3. Catalyst recyclability

The recycling efficiency of the TiHP catalyst was determined by demonstrating dehydration of fructose as a representative reaction. In this study, 500 mg fructose was reacted with 250 mg TiHP at 140 °C for 3 h water/THF solvent. After the 1st cycle, spent catalyst was separated by filtration, washed with water and dried. The recovered catalyst was then used for three more consecutive cycles in the similar fashion. The results show (Fig. 6) excellent recyclability of the catalyst up to the 4th cycle. Further characterizations of the recovered catalyst after the 3rd cycle suggest that the FTIR and powder XRD patterns of the recovered catalyst are similar to those of as-synthesized catalyst (Fig. 1a and b).

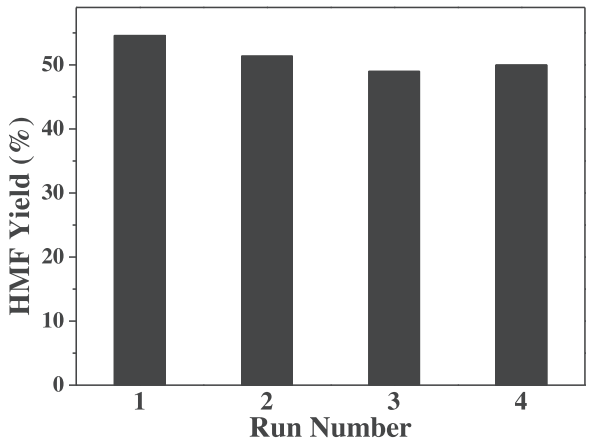

Fig. 6. Results of fructose dehydration using fresh and used TiHP catalyst. Fructose = 500 mg, TiHP = 250 mg, solvent = water (2 mL)/THF (10 mL), temperature = 140 °C and reaction time = 3 h. The aqueous phase contained 30 wt% NaCl.

4. Conclusion

The present report describes a simple method for the synthesis of template free TiHP catalyst containing dual acid sites. The material characteristics of as-synthesized TiHP have been elucidated using XRD, HR-TEM, FTIR, TGA/DTA, elemental analysis and NH_3-TPD methods. TGA/DTA data reveals the catalyst is stable up to 700 °C with only 6 wt% mass loss due to water of crystallization. FTIR data evidences the presence of phosphate group on the TiO_2 support and NH_3-TPD data confirms strong acidity (1.43 mmol g^{-1}). The activity of the TiHP catalyst has been investigated for dehydration of mono- (fructose, glucose, galactose) and disaccharides (cellobiose, maltose) in biphasic solvent (water/THF). Initial experiments reveal superior catalyst activity of the TiHP material for HMF production than that of TiO_2 precursor or a mixture of TiO_2/H_3PO_4. Reactions at higher temperatures or for longer time resulted in HMF rehydration product, LA to a significant extent which is due to the presence of Brønsted acid sites in the catalyst. Although individual Brønsted and Lewis acid densities look similar, higher HMF yields (55%) from fructose than that from glucose and galcatose suggests that the later reactions perhaps limited by the mass-transport of the catalyst. Therefore, these reactions in a larger reactor (2 L) having stronger stirring capability produced up to 35% HMF. Cellobiose and maltose conversions achieved 20 and 16% HMF, respectively. A slight difference in their reactivity could be due to difference in their hydrolysis rates owing to different glycosidic linkages. Recyclability study shows the catalyst retains activity up to the 4th cycles and the recovered catalyst has similar FTIR and XRD patterns as that of as-synthesized material. This catalyst may be further improved by varying the synthesis conditions in future to study of a facet dependent conversion of sugars and glycosidic polymers.

Acknowledgement

M.M.A.-O. acknowledges financial support from the Center for direct Catalytic Conversion of Biomass to Biofuels (C3Bio), an Energy Frontier Research Center funded by the U.S. Department of Energy, Office of Science, and Office of Basic Energy Sciences under Award Number DE-SC0000997. B.S. acknowledges the financial support from the Council of Scientific and Industrial Research (CSIR), India. I.A. and S.D. acknowledge CSIR and UGC, respectively for their research fellowship.

Appendix A. Supplementary data

Supplementary material related to this article can be found, in the online version, at http://dx.doi.org/10.1016/j.apcata.2014.08.019.

References

[1] A. Corma, S. Iborra, A. Velty, Chem. Rev. 107 (2007) 2411–2502.
[2] B. Kamm, Angew. Chem. Int. Ed. 46 (2007) 5056–5058.
[3] P. Gallezot, Chem. Soc. Rev. 41 (2012) 1538–1558.
[4] G.W. Huber, J. Chheda, C. Barret, J.A. Dumesic, Science 308 (2005) 1447–1450.
[5] R.J. van Putten, J.C. van der Waal, Ed. de Jong, C.B. Rasrendra, H.J. Heeres, J.G. de Vries, Chem. Rev. 113 (2013) 1499–1597.
[6] S. De, S. Dutta, S.B. Saha, Green Chem. 13 (2011) 2859–2868.
[7] S. Dutta, S. De, Md.I. Alam, M.M. Abu-Omar, B. Saha, J. Catal. 288 (2012) 8–15.
[8] Md.I. Alam, S. De, S. Dutta, B. Saha, RSC Adv. 2 (2012) 6890–6896.
[9] S. De, S. Dutta, A.K. Patra, A. Bhaumik, B. Saha, J. Mater. Chem. 21 (2011) 17505–17510.
[10] H.B. Zhao, J.E. Holladay, H. Brown, Z.C. Zhang, Science 316 (2007) 1597–1600.
[11] Y. Roman-Leshkov, J.N. Chheda, J.A. Dumesic, Science 312 (2006) 1933–1937.
[12] B. Saha, M.M. Abu-Omar, Green Chem. 16 (2014) 24–38.
[13] A. Chareonlimkun, V. Champreda, A. Shotipruk, N. Laosiripojana, Biores. Technol. 101 (2010) 4179–4186.
[14] M. Watanabe, Y. Aizawa, T. Iida, R. Nishimura, H. Inomata, Appl. Catal. A: Gen. 295 (2005) 150–156.
[15] D. Lai, L. Deng, Q. Guo, Y. Fu, Energy Environ. Sci. 4 (2011) 3552–3557.
[16] K. Shimizu, R. Uozumi, A. Satsuma, Catal. Commun. 10 (2009) 1849–1853.
[17] V.V. Ordomsky, J. van der Schaaf, J.C. Schouten, T.A. Nijhuis, J. Catal. 287 (2012) 68–75.
[18] X. Qi, M. Watanabe, T.M. Aida, R.L. Smith, Green Chem. 10 (2008) 799–805.
[19] D.J. Jones, G. Aptel, M. Brandhorst, M. Jacquin, J. Jimenez-Jimenez, A. Jimenez-Lopez, P. Maireles-Torres, I. Piwonski, E. Rodriguez-Castellon, J. Zajac, J. Roziere, J. Mater. Chem. 10 (2000) 1957–1963.
[20] Y. Zhang, J. Wang, J. Ren, X. Liu, X. Li, Y. Xia, G. Lu, Y. Wang, Catal. Sci. Technol. 2 (2012) 2485–2491.
[21] I. Jimenez-Morales, J. Santamaria-Gonzalez, P. Maireles-Torres, A. Jimenez-Lopez, Appl. Catal. B: Environ. 123–124 (2012) 316–323.
[22] A. Dutta, A.K. Patra, S. Dutta, B. Saha, A. Bhaumik, J. Mater. Chem. 22 (2012) 14094–14100.
[23] V.V. Ordomsky, J. van der Schaaf, J.C. Schouten, T.A. Nijhuis, ChemSusChem 5 (2012) 1812–1819.
[24] Y. Zhao, G. Zhu, X. Jiao, W. Liu, W. Pang, J. Mater. Chem. 10 (2000) 463–467.
[25] P. Cheng, R. Chen, J. Wang, J. Yu, T. Lan, W. Wang, H. Yang, H. Wu, C. Deng, Nanoscale Res. Lett. 5 (2010) 1313–1319.
[26] L. Korosi, S. Papp, I. Dekany, Chem. Mater. 22 (2010) 4356–4363.
[27] S. Ekambaram, S.C. Sevov, Angew. Chem. Int. Ed. 38 (1999) 372–375.
[28] Y. Liu, Z. Shi, L. Zhang, Y. Fu, J. Chen, B. Li, J. Hua, W. Pang, Chem. Mater. 13 (2001) 2017–2022.
[29] Z. Yin, Y. Sakamoto, J. Yu, S. Sun, O. Terasaki, R. Xu, J. Am. Chem. Soc. 126 (2004) 8882–8883.
[30] X.S. Li, A.R. Courtney, W. Yantasee, S.V. Mattigod, G.E. Fryxell, Inorg. Chem. Commun. 9 (2006) 293–295.
[31] A. Bhaumik, S. Iganaki, J. Am. Chem. Soc. 123 (2001) 691–696.
[32] M. DuBois, K. Gilles, J. Hamilton, P. Rebers, F. Smith, Anal. Chem. 28 (1956) 350–356.
[33] E.D. Dzyuba, V.V. Pechkovskii, G.I. Salonets, Zh. Prikl Spektrosk. 21 (1974) 127–131.
[34] L.R. Cumba, U.O. Bicalho, D.R. Carmo, Int. J. Electrochem. Sci. 7 (2012) 4465–4478.
[35] L.M. Nunes, C. Airoldi, Mater. Res. Bull. 34 (1999) 2121–2130.
[36] Y. Chudasama, J.A. Dumesic, Top. Catal. 52 (2009) 297–303.
[37] A. Dutta, D. Gupta, A.K. Patra, B. Saha, A. Bhaumik, ChemSusChem 7 (2013) 925–933.
[38] F.S. Asghari, H. Yoshida, Carbohydr. Res. 341 (2006) 2379–2387.
[39] P. Khemthong, P. Daorattanachai, N. Laosiripojana, K. Faungnawakij, Catal. Commun. 29 (2012) 96–100.
[40] Z. Zhang, Q. Wang, H. Xe, W. Liu, Z.K. Zhao, ChemSusChem 4 (2011) 131–138.
[41] R. Weingarten, J. Cho, R. Xing, W.C. Conner, G.W. Huber, ChemSusChem 5 (2012) 1280–1290.
[42] E. Nikolla, Y. Roman-Leshkov, M. Moliner, M.E. Davis, ACS Catal. 1 (2011) 408–411.
[43] Q. Zhao, L. Wang, S. Zhao, X. Wang, S. Wang, Fuel 90 (2011) 2289–2293.